Contents lists available at ScienceDirect

# Estuarine, Coastal and Shelf Science

# Fine-scale spatial distribution of the common lugworm *Arenicola marina*, and effects of intertidal clam fishing

CrossMark

Inna Boldina, Peter G. Beninger*

*Laboratoire de Biologie Marine, Faculté des Sciences, Université de Nantes, 2, rue de la Houssinière, 44322 Nantes, France*

**A B S T R A C T**

Despite its ubiquity and its role as an ecosystem engineer on temperate intertidal mudflats, little is known of the spatial ecology of the lugworm *Arenicola marina*. We estimated lugworm densities and analyzed the spatial distribution of *A. marina* on a French Atlantic mudflat subjected to long-term clam digging activities, and compared these to a nearby pristine reference mudflat, using a combination of geostatistical techniques: point-pattern analysis, autocorrelation, and wavelet analysis. Lugworm densities were an order of magnitude greater at the reference site. Although *A. marina* showed an aggregative spatial distribution at both sites, the characteristics and intensity of aggregation differed markedly between sites. The reference site showed an inhibition process (regular distribution) at distances <7.5 cm, whereas the impacted site showed a random distribution at this scale. At distances from 15 cm to several tens of meters, the spatial distribution of *A. marina* was clearly aggregated at both sites; however, the autocorrelation strength was much weaker at the impacted site. In addition, the non-impacted site presented multi-scale spatial distribution, which was not evident at the impacted site. The differences observed between the spatial distributions of the fishing-impacted vs. the non-impacted site reflect similar findings for other components of these two mudflat ecosystems, suggesting common community-level responses to prolonged mechanical perturbation: a decrease in naturally-occurring aggregation. This change may have consequences for basic biological characteristics such as reproduction, recruitment, growth, and feeding.

© 2014 Elsevier Ltd. All rights reserved.

## 1. Introduction

Temperate zone intertidal mudflats are characterized by high productivity and very dense populations of invertebrates (Whittaker, 1970; Pinckney and Zingmark, 1993; McLusky and Elliott, 2004; Kromkamp and Forster, 2006). They provide feeding and resting areas for large numbers of migratory shorebirds (Butler et al., 1987; Piersma and Jukema, 1990; Zwarts et al., 1990; Mawhinney et al., 1993), which feed on the meiofaunal and macrofaunal invertebrates (Piersma et al., 1998; Sutherland et al., 2000; Hamilton et al., 2006). Mudflats also provide nursery and feeding areas for commercially-important fish species (Gibson and Robb, 1992; Marshall and Elliott, 1997).

The deposit-feeding lugworm *Arenicola marina* is a dominant species of temperate-zone intertidal mudflats (Flach and Beukema, 1994), accounting for 10—20% of the total benthic biomass. Typical mean densities of 20—40 individuals m$^{-2}$ are found in the Wadden Sea, with relatively constant population densities (Beukema, 1976;

Volkenborn et al., 2007). An ecosystem engineer, *A. marina* transforms the intertidal mudflats habitat via bioturbation and its own physiological activity (Flach, 1992), consequently maintaining sediment permeability, stimulating nitrification (Hüttel, 1990), modifying carbon and sulfur dynamics (Kristensen, 2001; Nielsen et al., 2003) and inhibiting the succession to progressively finer sediment (Volkenborn et al., 2007). Bioturbation and feeding activities of *A. marina* also impact the biological community, e.g. meiofaunal and macrofaunal abundance and diversity (Flach, 1992, 1993; Volkenborn and Reise, 2006; Kuhnert et al., 2010), as well as microbial dynamics (Goñi-Urriza et al., 1999). *A. marina* is also used in pollution biomonitoring because of its bioaccumulation capacity (Casado-Martínez et al., 2007; Ramos-Gómez et al., 2011; Rodríguez-Romero et al., 2013).

Despite the importance of *Arenicola marina* in mudflat ecology, however, little is known concerning its spatial distribution within these habitats. Not only is spatial distribution one of the fundamental features of community organization, it is also essential to any serious sampling scheme in ecology (Legendre and Fortin, 1989; Underwood and Chapman, 1996; Fortin and Dale, 2005; Legendre and Legendre, 2012).

Through its production of distinctive fecal casts at the sediment surface, *Arenicola marina* is probably the most conspicuous infaunal invertebrate. Early studies reported a non-uniform spatial distribution of *A. marina*, based on qualitative visual determination (Chapman and Newell, 1949). Later studies reported an over-dispersed distribution pattern within 30 × 30 m squares (Flach and Beukema, 1994), using the inadequate variance: mean method (Hurlbert, 1990; Dale et al., 2002). More refined work using nearest-neighbor analysis concluded that *A. marina* was randomly distributed at a scale of 0.5 m$^2$ (Retraubun et al., 1996). It is thus evident that both the methodology and the knowledge of *A. marina* spatial distribution require clarification. To our knowledge, no study to date has investigated the fine-scale spatial structure of *A. marina* using modern geostatistical methods.

Due to its ubiquity on mudflats, *Arenicola marina* populations often overlap with those of fished infaunal molluscs, such as clams. The potential effects of clam fishing on the spatial structure of this ecosystem engineer have not been investigated to date. Although there have been attempts to evaluate the effect of harvesting and human trampling on the abundance of *A. marina* (Beukema et al., 1995; Cryer et al., 1987; Rossi et al., 2007), we are not aware of any study investigating the effect of anthropogenic mechanical perturbation on the fine-scale spatial structure of *A. marina*.

In the present study, we use modern geostatistical methods for analyzing the fine-scale spatial structure of an unperturbed *Arenicola marina* population, and compare this with a site impacted by long-term clam digging.

## 2. Materials and methods

### 2.1. Terminology

Due to the both the relative novelty of geo-statistical techniques in marine ecology, and the instability of terminology in spatial analysis (Fortin and Dale, 2005), it is necessary to explain some of the key terms used in this approach. The following glossary is intended to provide sufficient detail for understanding of the rationale for each procedure or concept; for complete background, we direct the reader to the following seminal works: Fortin and Dale (2005), Illian et al. (2008). The terms are presented in a logical, rather than an alphabetical, order.

**Spatial process** is the underlying biological process which produces an observed spatial pattern.

A **Stationary spatial process** is one which is constant (i.e. individual density means and variances are constant) throughout the studied region.

**Isotropic spatial process** designates a spatial process which is invariant in all directions.

**Spatial pattern** is the distribution of individuals in a given space, usually "…a 'single realization' or 'snapshot' of a process or of a combination of processes at one given time" (Fortin et al., 2003).

**Autocorrelation** is the correlation between data points themselves, rather than between data series. Autocorrelation may be positive (nearby points have more similar values than would be expected by random) and negative (nearby points have less similar values than would be expected by random). In the presence of autocorrelation sampled values are not independent from each other (Tobler, 1970). The kind of autocorrelation between values defines the type of spatial distribution.

**Aggregation** or aggregated (clustered, clumped, grouped) spatial distribution occurs when the spatial autocorrelation is positive, so individuals tend to occur in groups rather than in a random spatial distribution.

**Inhibition** or uniform (regular) spatial distribution occurs when the spatial autocorrelation is negative; individuals repel each other,

maximizing the distance between themselves, so they are spaced more evenly than in a random spatial distribution.

**Point pattern analysis** studies the spatial distribution of individuals. Each point represents the position of individual.

**First-order point pattern analysis** is based on the density of points (individuals) across the studied area.

**Second-order point pattern analysis** is based on the distances between points across the studied area.

**Kernel density estimation** may be likened to a histogram based on probabilities rather than on data points.

**Ripley's K** is a function based on the comparison of average point density (i.e. density of individual animals) in a given area to average point density of circles of increasing radii, drawn around each data point, within this area (Fig. 1).

The average density of points within circles of increasing radius *r* is compared to the average point density of the total area (Fortin and Dale, 2005):

$$K(r) = \frac{1}{n} \sum_{i=1}^{n} Np_i(r)/\lambda$$

where $p_i$ is the $i$-th point, and $\lambda$ is the average density of points.

Ripley's K values vs. *r* plots reveal the inter-point distances where the spatial aggregation is statistically significant by comparing the actual K values with the K values of a random spatial point pattern of the same size and shape, simulated using a Monte Carlo method. An aggregated spatial distribution is present when the Ripley's K values of the data set are located above the simulated envelope of random point data. Ripley's K values located within the simulated envelope indicate a random spatial distribution, and Ripley's K values situated below the simulated envelope indicate a regular spatial distribution, itself indicative of inhibition (Illian et al., 2008). Since Ripley's K values may be biased at the edges of studied areas, an edge correction of Ripley's K is conventionally used (Illian et al., 2008).

**Quadrat-based count data** are obtained by dividing the studied area into quadrats, in which the number of individuals is counted (contrast with point pattern data, where individual data points are used). The obtained data may be analyzed with different geo-statistical methods, such as Moran's *I* correlograms, wavelets etc.
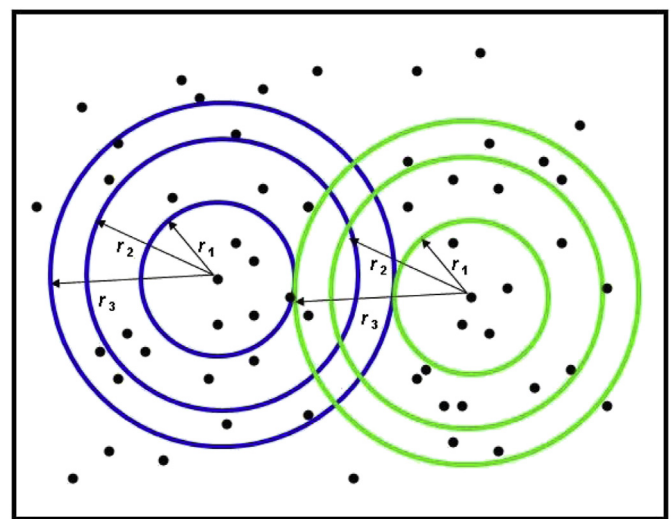


**Fig. 1.** Construction of a Ripley's K function. The circles of different radii ($r_1$, $r_2$, $r_3$ …) are drawn around every point (individual) of the studied area. For purposes of illustration, only three concentric circles drawn around two points are illustrated here.
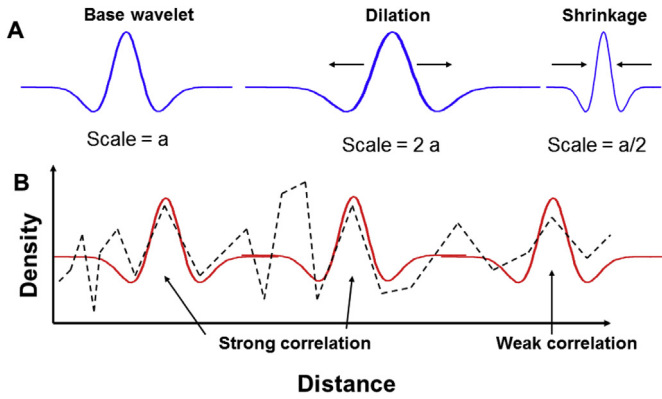
Fig. 2. A. Example of base wavelet (Mexican hat wavelet) with different scale factors (dilations). The most compressed wavelet corresponds to the smallest scale factor. B. Example of correlation between the spatial process (*i.e.* density variation) and the base wavelet at a given scale.

**Moran's *I* autocorrelation coefficient** may be considered an extension of the familiar Pearson correlation coefficient; it measures autocorrelation (Legendre and Legendre, 2012). Autocorrelograms are plots of Moran's *I* vs. distance.

**Distance class** is a mathematical construct obtained from the data after the study, in order to produce optimal-resolution autocorrelograms.

### 2.1.1. Hierarchical spatial structure

A spatial process may be structured at different scales. The study of a spatial process at different levels of resolution permits its hierarchical (scale-related) representation.

### 2.1.2. Wavelets

Wavelet analysis defines spatial structure as a function of scale and position (Daubechies, 1988). The wavelet is a mathematical function with limited duration and an average value of zero. Each base wavelet may be stretched or shrunk (Fig. 2A). The wavelet dilation defines its scale. The wavelet function is then shifted over the data function at various scales (Bradshaw and Spies, 1992; Flandrin et al., 2010). If the wavelet function matches the data well (similar shape and dimension), the absolute value of the co-efficients of wavelet transformation is high, and it is low when the wavelet and data functions do not match well (Fig.2B).

### 2.2. Study locations and sampling dates

Two study sites were located in Bourgneuf Bay on the French Atlantic coast (Fig.3). The impacted study site, situated at 46.932°N, − 2.126°W, has been heavily exploited year-round by recreational clam diggers since the 1990's (Hitier et al., 2010) and probably since the construction of a submersible paved road in 1939 and the end of WWII. The annual mean number of visits to this site is nearly 40.000 (unpublished data, in preparation). The non-impacted site, located nearby at 46.973°N, − 2.186 °W, was accessible only by boat, and thus out of the reach of recreational clam diggers; it is classified as a non-exploited site (Hitier et al., 2010). Although *Arenicola marina* may be used as bait for sport fishing, we did not encounter any bait-digging over the 2.5 years of our sampling program. Furthermore, a separate aspect of this program involved personal polling of 422 intertidal fishers on the impacted mudflat; none of the fishers polled had targeted *A. marina*. Any anthropogenic harvesting of *A. marina* is thus negligible.

The intertidal sediment characteristics, depths, and salinities of the two sampling sites were quite similar, with a semidiurnal macrotidal cycle, high turbidity, seasonally variable water temperatures between 4.4 °C and 20.4 °C, and seasonally variable salinity from 30 to 31. Sediment profiles were obtained from 6 sediment cores to a depth of 5 cm, using laser granulometry and Gradistat software (Bott and Pye, 2001). Both sites were characterized by medium sand sediment (using the size scale of Bott and Pye (2001)), with very little difference in profile (Table 1).

Sampling was conducted at low tide on 8 May and 25 June 2012 for the non-impacted site and 22 June 2012 for the impacted site. As the spatial distribution characteristics proved to be nearly identical
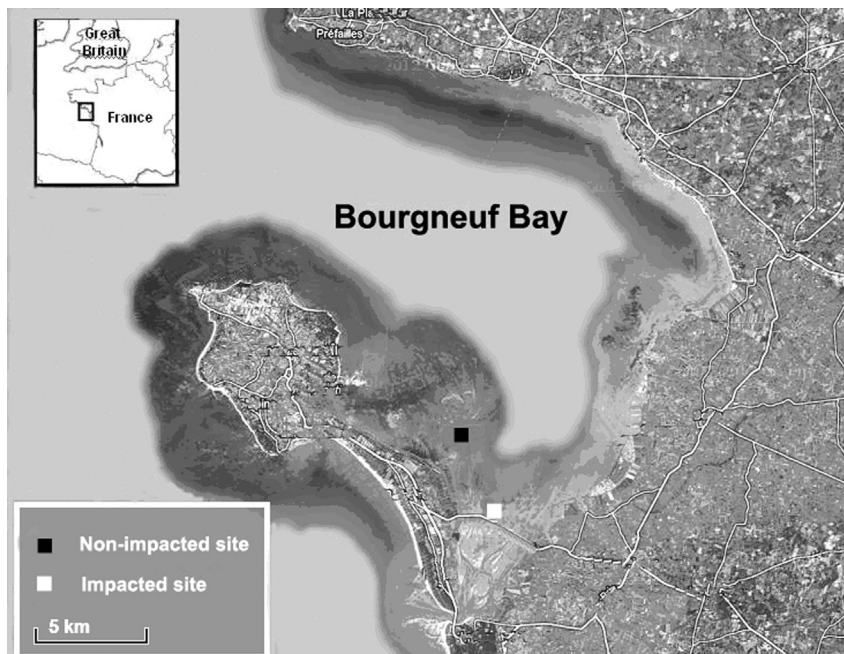


Fig. 3. Location of the two study sites in Bourgneuf Bay, France.

**Table 1**
Characteristics of the two investigated sites and their sediments.

| Characteristics | Non-impacted site | Impacted site |
|---|---|---|
| Temperature | 4.5–24.5 °C | 4.5–24.5 °C |
| Salinity | 30–31 | 30–31 |
| Depth (m)[*] | 3.1 | 3.0 |
| Sediments | | |
|   Mean diameter μm | 372.1 ± 24.3 | 415 ± 20.3 |
|   Sorting | Moderate | Moderate |
| Sediment fractions % | | |
| Mud (<63 μm) | 1.3 ± 0.3 | 0.8 ± 0.1 |
| V. fine sand (63 μm–125 μm) | 1.1 ± 0.5 | 0.4 ± 0.3 |
| Fine sand (125 μm–250 μm) | 26.1 ± 8.1 | 15.5 ± 6.2 |
| Medium sand (250 μm–500 μm) | 52.1 ± 9.2 | 59.7 ± 9.5 |
| Coarse sand (500 μm–1 mm) | 23.1 ± 12.5 | 28.4 ± 7.7 |

[*] Depth at high tide, coefficient 120 (http://www.geoportail.gouv.fr).

for the two sampling dates at the non-impacted site, we present the results only for 25 June 2012 for this site.

In order to investigate the potential effect of long-term intertidal clam fishing on the spatial distribution of *Arenicola marina*, it was necessary to investigate soft-bottom intertidal sites which were comparable in most respects except for anthropogenic impact. Ideally, in a study of the eventual ecological impact of intertidal fishing, several impacted sites should be compared with several non-impacted sites, to control for site-specific effects. However, it is sometimes impossible to find multiple non-impacted sites (e.g. Brown and Herbert Wilson Jr. (1997), present study). In such cases, when replication is not feasible but the effect size is likely to be large, clear demonstration of this effect may be considered an indication of real effect (Oksanen, 2001; Cleary, 2003). Despite ubiquitous and frequent intertidal fishing activity on the French Atlantic coast, in the present study we were able to locate a site which was not fished intertidally because it was not accessible on foot, and was too small to be profitably fished by professional clam diggers. We thus compared a fishing-impacted site with a non-impacted site.

### 2.3. Sampling strategy

*Arenicola marina* lives in J-shaped burrows which extend from 20 to 40 cm into the sediment (Fig. 4). Sediment is ingested by the worm and defecated as characteristic fecal mounds at the sediment surface above the tail shaft of the burrow (Riisgård and Banta, 1998).

Overlapping low oblique photographs of the surface sediment (approx. 3.5 m$^2$) were taken along each transect parallel to the tidal flow. Individual positions were identified by fecal casts (Fig.4). This method for the estimation of lugworm densities was confirmed to

be reliable in previous studies (Flach and Beukema, 1994; Volkenborn et al., 2007). Scale rectification of oblique photographs was performed using reference bars placed directly on the sediment surface. Cartesian coordinates of each fecal cast were identified and transformed to real field coordinates using scale rectification (Chandler et al., 2005). A band corresponding to 25 field cm was removed from the edge of each image, to compensate for lens distortion. The total area analyzed at each site was nearly 87 m$^2$.

### 2.4. Test for isotropy

Perpendicular transects were performed for verification of isotropy, as per Boldina and Beninger (2013). The spatial distributions were isotropic within the intertidal zone, so the data from all transects were grouped and analyzed together.

### 2.5. Statistical analysis

#### 2.5.1. Second-order point pattern analysis

Analysis of spatial distribution is a process akin to successive approximation: different techniques may be used, and the technique or combination of techniques which allows the most complete description is then retained. The first approach used in the present study was based on point pattern analysis. A spatial point pattern is a set of points which can be identified by their co-ordinates within a chosen region of space. We used a second-order point pattern analysis based on Ripley's K function (Ripley, 1976).

In order to stabilize the variance and facilitate interpretation, we used the following transformation of the K function: L function (Besag, 1977):

$$L(r) = \sqrt{K(r)/\pi}$$

We also computed the pair correlation function (PCF) which is a modification of the Ripley's K function (Stoyan et al., 1995):

$$PCF = \frac{1}{2\pi r} \frac{dK(r)}{dr}$$

where $dK(r)/dr$ is the derivative of $K(r)$.

The Ripley's K function and its derivative, the Besag's L function, measure the spatial association within areas delimited by circles, whereas the PCF measures the association within rings. Whereas Ripley's K analysis may give less reliable results for large $r$, as they are considerably influenced by the associations at the smaller $r$, PCF is free of this influence (Perry et al., 2006). PCF = 1 indicates a random spatial point pattern, PCF > 1 indicates spatial aggregation, and PCF < 1 is consistent with a regular distribution (Baddeley and Turner, 2005).
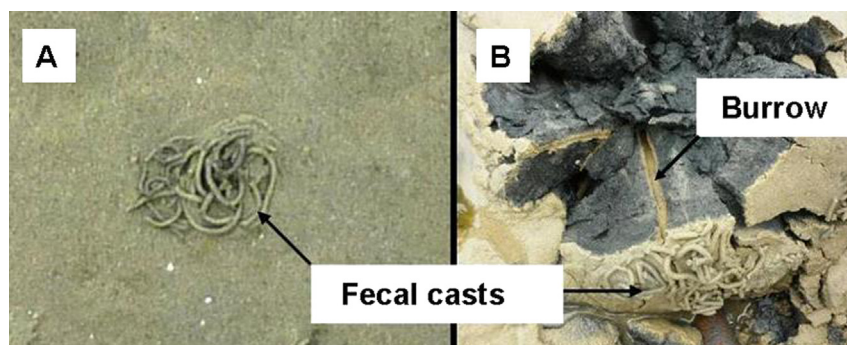


**Fig. 4.** *A. marina* fecal casts at sediment surface (A) and sub-surface burrow (B).

Ripley's K, Besag's L and PCF functions are only valid for stationary spatial processes. It was therefore necessary, prior to analysis, to verify the stationarity assumption (Illian et al., 2008), which was done using Gaussian kernel smoothing (Baddeley and Turner, 2005).

### 2.5.2. Spatial analysis on quadrat count data

When a rectangular sampling area is used for point pattern analyses (as in the linearly-arranged images of the present study) the $r$ should not exceed ¼ of the smallest side of the rectangle (Baddeley and Turner, 2005). In our case, this limitation means that the Ripley's K, Besag's L and PCF functions could only be used for distances <50 cm. In order to characterize spatial distribution at larger scales, we converted the point process data to quadrat-count data. The studied area was divided into contiguous 35 × 35 cm quadrats, and the number of points within each quadrat was defined. Two complementary geostatistical techniques were used for the quadrat-count data: Moran's $I$ spatial autocorrelation and wavelet analyses.

Although the quadrat-count data transformation results in partial loss of information (Perry et al., 2002) and the inability to evaluate interactions at $r$-values less than the side length of the quadrats, the combination of second-order point pattern analysis, Moran's $I$ spatial autocorrelation and wavelets techniques allows the fullest possible description of spatial distribution over scales from a few cm to tens of meters. At distances ≤50 cm, the second-order point pattern analysis (L and PCF functions) elucidates the type and characteristics of spatial distribution. Finer detail of spatial characteristics, such as information about hierarchical structure, may be obtained through wavelet analysis, allowing multi-resolution and identification of the dominant scale of pattern (Percival, 1995; Fortin et al., 2012). Wavelet analysis may thus be a useful complementary method to traditional geostatistical methods (Bradshaw and Spies, 1992).

### 2.5.3. Moran's I spatial autocorrelation analysis

Before constructing the spatial autocorrelograms, the quadrat count data were grouped into 20 distance classes of equal size, and Moran's $I$ autocorrelation coefficient was computed for each distance class (Dale et al., 2002). Spatial autocorrelograms were constructed by plotting the lag distances vs. the corresponding Moran's $I$ values (Fortin et al., 2002; Fortin and Dale, 2005). The statistical significance of the value of Moran's $I$ obtained for each distance class was assessed by the Monte Carlo permutation test (Besag and Diggle, 1977; Diggle, 2003; Legendre and Legendre, 2012). The spatial range (patch size) was set at the distance that corresponded to the Moran's $I$ 0-value (Sandulli and Pinckney, 1999; Fortin and Dale, 2005).

### 2.5.4. Wavelet analysis

Wavelet analysis was also applied to the quadrat-count data (for background in this technique, see Bradshaw and Spies (1992); Dale and Mah (1998); Torrence and Compo (1998); Broughton and Bryan (2008); Cazelles et al. (2008)). As a wavelet transformation is a function of both scale and location, the results may be difficult to interpret, especially for a complex spatial structure with nested patterns. A refinement termed the wavelet variance function facilitates the interpretation of multi-scale spatial pattern (Bradshaw and Spies, 1992; Percival, 1995). A scalogram plots wavelet variance vs. scale (Torrence and Compo, 1998). The peak in wavelet variance corresponds to the scale of the dominant pattern in the data, and the height of this peak indicates how much each scale contributes to the overall pattern (Bradshaw and Spies, 1992; Dale and Mah, 1998).

Different wavelet functions may be chosen for the analysis. This choice depends on the type of analyzed data and the hypothesized pattern, but remains arbitrary. The best fit pattern for the *Arenicola marina* densities was found to be the French hat wavelet (Dale and Mah, 1998; Dale, 2000).

Point pattern analyses were conducted with the R spatstat package (Baddeley and Turner, 2005), and autocorrelation analysis with the R ncf package (Bjørnstad, 2006). Wavelet analysis was performed using Passage software (Rosenberg and Anderson, 2011).

## 3. Results

### 3.1. Testing for spatial homogeneity of studied areas

No trend in spatial data was apparent at either site (Fig. 5 A and B). We may thus consider that the studied spatial process is stationary, and that both L and PCF functions may be used for data analysis.

The mean density of *Arenicola marina* was 22.82 individuals m$^{-2}$ at the non-impacted site and 2.60 individuals m$^{-2}$ at the impacted site.

### 3.2. Spatial point pattern analysis

#### 3.2.1. Non-impacted site

For the non-impacted site, the values of the L-function for the distances from approximately 2.5–7.5 cm are situated below the 95% confidence envelope, indicating an inhibition at these distances. For distances from 7.5 to 9.5 cm, the values of the L-function situated within the 95% simulation envelope indicate a random distribution, and for distances greater than 9.5 cm the spatial pattern becomes clustered, with L-function values situated above the upper 95% confidence envelope (Fig 6).

Significant deviations from a random pattern were also detected on the pair correlated function plot (Fig. 7). The presence of an inhibition process is clearly visible for the values of PCF <1 for distances less than 5.5 cm. The spatial process appears clustered at larger scales.

#### 3.2.2. Impacted site

At the impacted site, the spatial distribution for distances <15 cm appears random (L-function values within the 95% confidence envelope). For distances greater than 15 cm, the spatial pattern appears to be clustered (L-functions values above the 95% confidence envelope) (Fig.8 A). Nevertheless, the L-function values are situated very close to the values of the simulation envelope, and thus should be interpreted with caution (Loosmore and Ford, 2006;
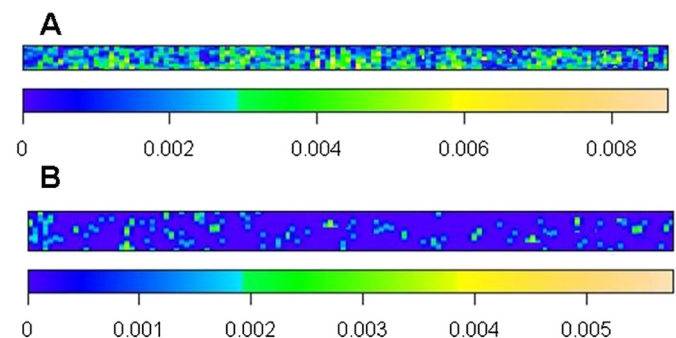


**Fig. 5.** Test for presence of visible spatial trend with Kernel density estimation of *A. marina*. A. Non-impacted site. Bandwidth = 10. B. Impacted site. Bandwidth = 5.
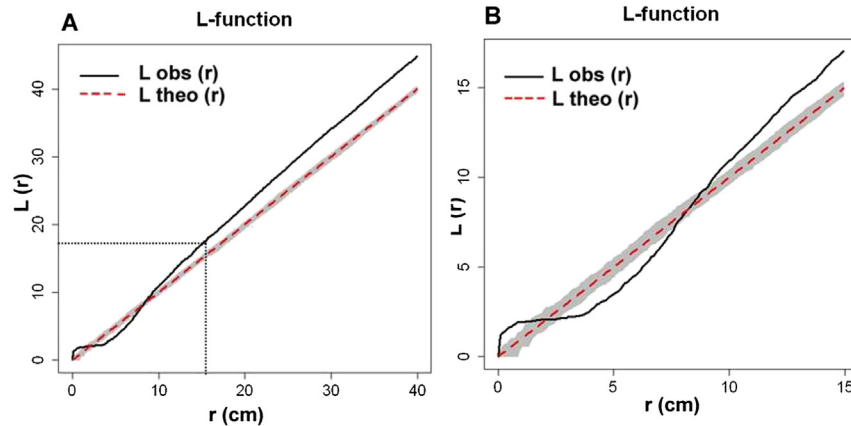
**Fig. 6.** Non-impacted site. A. Besag's L-function for the *A. marina* spatial distribution. Dotted framed area is shown in B: detail of Besag's L-function for the *A. marina* spatial distribution, 0–15 cm. The solid line corresponds to the estimated function. The dashed line represents the corresponding random spatial point process. Gray areas define the 95% confidence envelope under the null hypothesis of spatial randomness, computed by Monte Carlo simulation using 199 replicates.

Blanco et al., 2008). The plot of the pair correlation function shows spatial aggregation at distances >8 cm (Fig. 8 B).

### 3.3. Autocorrelation analyses for quadrat-count transformed data

#### 3.3.1. Non-impacted site

The spatial autocorrelogram for *Arenicola marina* for the non-impacted site demonstrates strong autocorrelation with maximum and minimum Moran's $I$ values of 0.39 and −0.38 (Fig.9 A.). The Moran's $I$ values were statistically significant for all distance classes except the $5^{th}$ and the largest distance classes. The spatial autocorrelation was positive for distances less than 14 m, and negative for distances between 14 and 46 m. The patch size was therefore 14 m. The presence of the second peak on the correlogram, at a distance of approximately 50 m, indicates that there was more than one patch detected within the sampled area (Fortin and Dale, 2005).
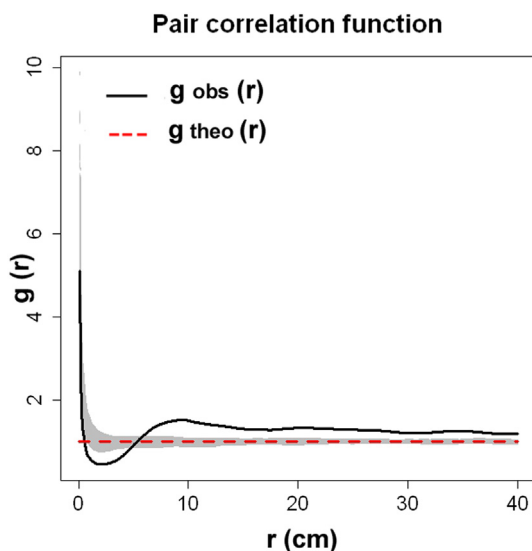


**Fig. 7.** Non-impacted site. Pair correlation function for the A. *marina* spatial distribution. The solid line corresponds to the estimated function; the dashed line represents the corresponding random spatial point process; gray areas define the 95% confidence envelope under the null hypothesis of spatial randomness, computed by Monte Carlo simulation using 199 replicates.

#### 3.3.2. Impacted site

The spatial autocorrelogram for *Arenicola marina* for the impacted site demonstrates autocorrelation with maximum and minimum Moran's $I$ values of 0.2 and −0.23 (Fig.9 B). The spatial autocorrelation was positive for distances less than 9 m, and negative for the distances between 9 and 29.5 m. The patch size was therefore 9 m.

### 3.4. Wavelet analysis for quadrat-count data

#### 3.4.1. Non-impacted site

A clear repeating spatial pattern is observed on the wavelet scalogram for the non-impacted site (Fig.10 A). This repeating pattern corresponds to the distances of approximately 7.7 m, 15.75 m, 26.25 m, 35 m and 42 m (quadrat numbers × 0.35 m). The wavelet variance has high values across all tested spatial scales (Fig.10 B). The strongest peak at scale 2 (0.7 m) (scale × 0.35 m) indicates the dominant scale (i.e. greatest contribution to the overall spatial pattern). The presence of peaks at scales 4 (1.40 m) and 6 (2.10 m) show that these two scales also contribute, albeit to a lesser extent (since the wavelet variance at these scales is weaker), to the global spatial structure. In summary, the wavelet analysis indicates that the spatial distribution of *Arenicola marina* at the non-impacted site is characterized by several high-intensity scales of patchiness, with a dominant fine scale.

#### 3.4.2. Impacted site

No clear spatial pattern can be detected from the scalogram for the impacted site (Fig. 10 C). Wavelet variance was much lower at the impacted site compared to the non-impacted site, and decreased across the tested scales. Distinct peaks were observed only at scales 1 (0.35 m) and 2 (0.7 m), which means that, contrary to the non-impacted site, the spatial structure of *Arenicola marina* at the impacted site did not present a multi-scale pattern.

## 4. Discussion

The combined approach using point pattern analysis, autocorrelation, and wavelet analysis allowed a thorough characterization of the spatial distribution of *Arenicola marina* at several scales, from cm to tens of meters. At distances <7.5 cm, an inhibition process appears to operate at the non-impacted site. This fine-scale inhibition process may be due to the bioturbation and feeding activities of *A. marina* (Flach, 1992; Flach and de Bruin, 1993; Flach and
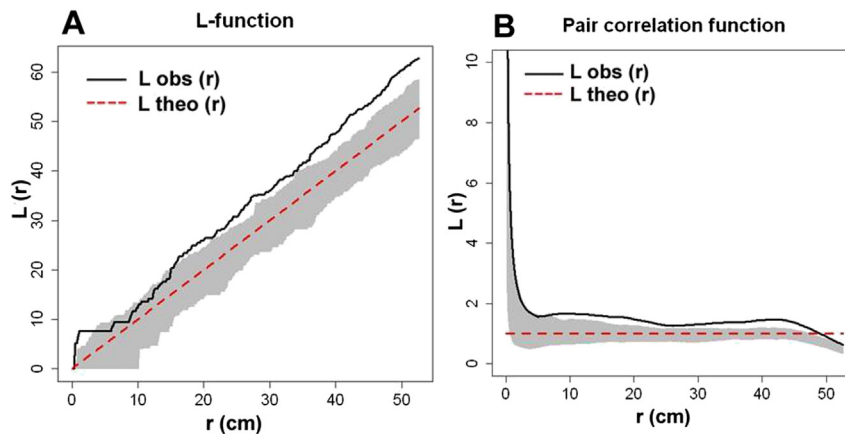
**Fig. 8.** Impacted site. A. Besag's L-function for the *A. marina* spatial distribution. B. Pair correlation function for the *A. marina* spatial distribution. The solid line corresponds to the estimated function. The dashed line represents the corresponding random spatial point process. Gray area defines the 95% confidence envelope under the null hypothesis of spatial randomness, computed by Monte Carlo simulation using 199 replicates.

Beukema, 1994). Deposivores feed from a limited circumferential area, from which conspecifics are excluded, probably due to recruitment interference (Flach, 1993) (Rijken, 1979). Deposivores, such as *A. marina*, therefore present a more dispersed fine-scale distribution than suspensivores (Flach and Beukema, 1994). Indeed, the sympatric bivalve suspensivore *Cerastoderma edule* displayed a definite fine-scale aggregated distribution (Boldina and Beninger, 2013).

Fine-scale inhibition was not observed at the impacted site, and indeed the spatial distribution appeared random for distances <15 cm. The absence of inhibition at this site may be due to the reduced density of *Arenicola marina*, generating a less structured distribution in the absence of competition for food.

At distances from 15 cm to several tens of meters, the distribution of *Arenicola marina* was aggregated at both sites. This change in the type of spatial distribution may be due to the different processes governing spatial structure at this scale. When competition



**Fig. 9.** All-directional spatial autocorrelogram for quadrat-count transformed data using 20 equidistant classes. Statistically significant values are represented by black symbols; non-significant values are represented by empty symbols. A. Non-impacted site. B. Impacted site.

for food is no longer a determining factor, the formation of spatial patterns may be determined by larval settlement and post-settlement processes. Settlement itself is not random (Woodin et al., 1995), and is influenced by several factors. The reproductive success of *A. marina* depends at least partly on the density of adult individuals, which facilitates pheromone-mediated synchronized spawning (Hardege et al., 1996; Hardege and Bentley, 1997; Watson et al., 2003), so the importance of an aggregative spatial distribution is obvious.

Although the spatial distribution at distances >15 cm was clearly aggregated at both sites, the strength of autocorrelation was much weaker at the impacted site. Furthermore, the non-impacted site presents multi-scale spatial distribution, which was not evident at the impacted site. Homogenization of spatial structure on the impacted site may be due to the capacity of post-larval juveniles of *Arenicola marina* to discriminate between disturbed and undisturbed sediment. Woodin et al. (1995) showed that juveniles of *A. marina* avoid burrowing in disturbed sediment and may be entrained by currents. A similar decrease in the strength of spatial aggregation, accompanied by spatial homogenization, at the impacted site was observed both for the targeted species *Cerastoderma edule* (Boldina and Beninger, 2013) and *Tapes philippinarum* (in preparation), as well as for the meiofauna (Boldina et al., 2014). A decrease in the strength of spatial aggregation and an increase in homogenization thus appear to be characteristic consequences of long-term clam fishing for each of the compartments studied, and may be early indicators of ecological destabilization. A much more conspicuous indicator of the impact of prolonged mechanical disturbance is the comparative densities of *A. marina*, which were an order of magnitude lower at the site subjected to clam fishing and associated human trampling. Such a difference in density suggests that long-term recreational clam digging has an astonishingly severe impact on the density of this ecosystem engineer, since even in areas subjected to heavily-mechanized lugworm harvesting, only a twofold decrease in lugworm density has been observed (Beukema, 1995).

The results of the present study concerning the effects of intertidal clam fishing on non-target species are congruent with those of previous investigations on ship-based benthic fishing activities, which indicated negative effects of mechanical disturbance (Veale et al., 2000; Jennings et al., 2001; Piersma et al., 2001; Jennings et al., 2002; Hermsen et al., 2003; Hixon and Tissot, 2007; Shephard et al., 2010; Lambert et al., 2011; Smith et al., 2013), and with the few studies on mechanical disturbance on
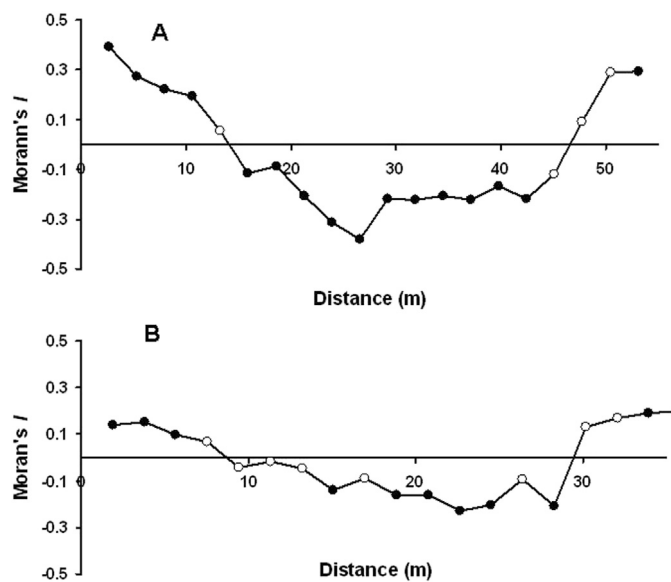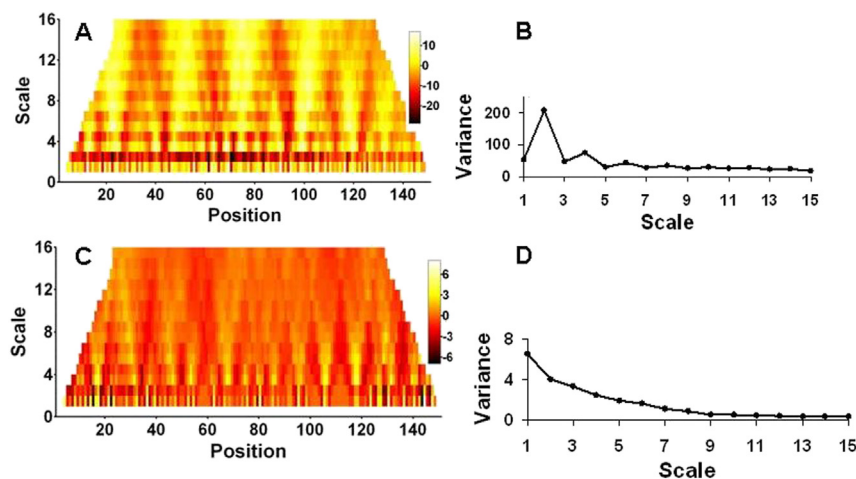
**Fig. 10.** Wavelet analysis for quadrat count data of *A. marina*. A. French hat wavelet transformation for *A. marina* densities. Non-impacted site. Horizontal axis corresponds to the quadrat number. Each quadrat numbered on the horizontal axis had a side length of 35 cm; transect distances in cm may be obtained by multiplying the quadrat number by 35. B. Wavelet variance of *A. marina* densities, non-impacted site. C. French hat wavelet transformation for *A. marina* densities, impacted site. D. Wavelet variance of *A. marina* densities, impacted site.

intertidal mudflats (Beukema, 1995; Griffiths et al., 2006; Rossi et al., 2007). In light of emerging ecological theory concerning the effects of persistent human disturbance on vulnerability to ecosystem collapse (MacDougall et al., 2013), and the uncertainty of long-term target species population dynamics under situations of fishery-induced selection (e.g. for large-size individuals, as in the intertidal clam fishery) or over-exploitation (Salinas et al., 2012; Neubauer et al., 2013), the present study highlights the need for enhanced attention to the heretofore largely neglected activity of intertidal mudflat clam fishing.

The regulatory aspects of intertidal fishing are highly variable, even within jurisdictions (Cosqueric-Boldina, 2011). Quotas, minimum sizes, fishing seasons, permits, and gear restrictions are the main regulatory instruments. From the foregoing, the effect of periodic closures to intertidal fishing could be ascertained. While such a measure would probably increase the density of *Arenicola marina*, it might also restore the species-specific spatial distributions in these areas, albeit slowly (Beukema, 1995). The question of enforcement is obviously crucial to any such measure, and likely to be a weakness in countries with a long history of virtually unimpeded recreational access to the resource, such as France.

### References

Baddeley, A., Turner, R., 2005. Spatstat: an R package for analyzing spatial point patterns. J. Stat. Softw. 12, 1–42.
Besag, J., 1977. Comments on Ripley's paper. J. R. Stat. Soc. Ser. 39, 193–195.
Besag, J.P., Diggle, J., 1977. Simple Monte Carlo tests for spatial pattern. Appl. Stat. 26, 327–333.
Beukema, J.J., 1976. Biomass and species richness of the macro-bentic animals living in the tidal flats of the Dutch Wadden Sea. Neth. J. Sea Res. 10, 236–261.
Beukema, J.J., 1995. Long-term effects of mechanical harvesting of lugworms *Arenicola marina* on the zoobenthic community of a tidal flat in the Wadden Sea. Neth. J. Sea Res. 219, 219–227.
Bjørnstad, O.N., 2006. Package 'ncf ': Spatial Nonparametric Covariance Functions.
Blanco, P.D., Rostagno, C.M., del Valle, H.F., Beeskow, A.M., Wiegand, T., 2008. Grazing impacts in vegetated dune fields: predictions from spatial pattern analysis. Rangel. Ecol. Manag. 61, 194–203.

Boldina, I., Beninger, P.G., 2013. Fine-scale spatial structure of the exploited infaunal bivalve *Cerastoderma edule* on the French Atlantic coast. J. Sea Res. 76, 193–200.
Boldina, I., Beninger, P.G., Le Coz, M., 2014. Effect of long-term mechanical perturbation on intertidal soft-bottom meiofaunal community spatial structure. J. Sea Res. 85, 85–91.
Bott, S., Pye, K., 2001. Gradistat: a grain size distribution and statistics package for the analysis of unconsolidated sediments. Earth Surf. Process. Landf. 26, 1237–1248.
Bradshaw, G.A., Spies, T.A., 1992. Characterizing canopy gap structure in forests using wavelet analysis. J. Ecol. 80, 205–215.
Broughton, S.A., Bryan, K.M., 2008. Discrete Fourier Analysis and Wavelets: Applications to Signal and Image Processing. Wiley-Interscience, 360 pp.
Brown, B., Herbert Wilson Jr., W., 1997. The role of commercial digging of mudflats as an agent for change of infaunal intertidal populations. J. Exp. Mar. Biol. Ecol. 218, 49–61.
Butler, R.W., Kaiser, G.W., Smith, G.E.J., 1987. Migration chronology, length of stay, sex ratio, and weight of western sandpipers, (Calidris mauri) on the south coast of British Columbia. J. Field Ornithol. 58, 103–111.
Casado-Martínez, M.C., Fernández, N., Forja, J.M., DelValls, T.A., 2007. Liquid versus solid phase bioassays for dredged material toxicity assessment. Environ. Int. 33, 456–462.
Cazelles, B., Chavez, M., Berteaux, D., Ménard, F., Vik, J., Jenouvrier, S., Stenseth, N., 2008. Wavelet analysis of ecological time series. Oecologia 156, 287–304.
Chandler, J.H., Fryer, J.G., Amanda, J., 2005. Metric capabilities of low-cost digital cameras for close range surface measurement. Photogramm. Rec. 20, 12–26.
Chapman, G., Newell, G., 1949. The distribution of lugworms (*Arenicola marina* L.) over the flats at Whistable. J. Mar. Biolog. Assoc. U.K. 28, 627–634.
Cleary, D.R., 2003. An examination of scale of assessment, logging and ENSO-induced fires on butterfly diversity in Borneo. Oecologia 135, 313–321.
Cosqueric-Boldina, I., 2011. Cadre juridique des activités de pêche à pied des coquillages sur le littoral atlantique français. Annu. Droit Marit. Océaniq. XXIX, 145–181.
Cryer, M.C., Whittle, G.N., Williams, R., 1987. The impact of bait collection by anglers on marine intertidal invertebrates. Biol. Conserv 42, 83–93.
Dale, M.R.T., 2000. Spatial Pattern Analysis in Plant Ecology. Cambridge University Press, 326 pp.
Dale, M.R.T., Dixon, P., Fortin, M.-J., Legendre, P., Myers, D.E., Rosenberg, M.S., 2002. Conceptual and mathematical relationships among methods for spatial analysis. Ecography 25, 558–577.
Dale, M.R.T., Mah, M., 1998. The use of wavelets for spatial pattern analysis in ecology. J. Veg. Sci. 9, 805–814.
Daubechies, I., 1988. Orthonormal bases of compactly supported wavelets. Commun. Pure Appl. Math. 41, 909–996.
Diggle, P.J., 2003. Statistical Analysis of Spatial Point Patterns. Hodder Education Publishers, 159 pp.
Flach, E.C., 1992. Disturbance of benthic infauna by sediment-reworking activities of the lugworm *Arenicola marina*. Neth. J. Sea Res. 30, 81–89.
Flach, E.C., 1993. The distribution of the amphipod *Corophium arenarium* in the Dutch Wadden Sea: relationships with sediment composition and the presence of cockles and lugworms. Neth. J. Sea Res. 31, 281–290.
Flach, E.C., Beukema, J.J., 1994. Density-governing mechanisms in populations of the lugworm *Arenicola marina* on tidal flats. Mar. Ecol. Prog. Ser. 115, 139–149.
Flach, E.C., de Bruin, W., 1993. Effects of *Arenicola marina* and *Cerastoderma edule* on distribution, abundance and population structure of *Corophium volutator* in Gullmarsfjorden western Sweden. Sarsia 78, 105–118.

Flandrin, P., Gonçalves, P., Abry, P., 2010. Scale invariance and wavelets. In: Abry, P., Gonçalves, P., Véhel, J.L. (Eds.), Scaling, Fractals and Wavelets. ISTE, pp. 71–102.

Fortin, M.-J., Dale, M.R.T., 2005. Spatial Analysis: a Guide for Ecologists. Cambridge University Press, Cambridge, 365 pp.

Fortin, M.-J., Dale, M.R.T., ver Hoef, J., 2002. Spatial analysis in ecology. In: El-Shaarawi, A.H., Piegorsch, W.W. (Eds.), Encyclopedia of Environmetrics. Wiley, Chichester, pp. 2051–2058.

Fortin, M.-J., Boots, B., Csillag, F., Remmel, T.K., 2003. On the role of spatial stochastic models in understanding landscape indices in ecology. Oikos 102, 203–212.

Fortin, M.-J., James, P.M.A., MacKenzie, A., Melles, S.J., Rayfield, B., 2012. Spatial statistics, spatial regression, and graph theory in ecology. Spat. Stat. 1, 100–109.

Gibson, R.N., Robb, L., 1992. The relationship between body size, sediment grain size and the burying ability of juvenile plaice, Pleuronectes platessa. J. Fish. Biology 40, 771–778.

Goñi-Urriza, M., de Montaudouin, X., Guyoneaud, R., Bachelet, G., de Wit, R., 1999. Effect of macrofaunal bioturbation on bacterial distribution in marine sandy sediments, with special reference to sulphur-oxidising bacteria. J. Sea Res. 41, 269–279.

Griffiths, J., Dethier, M., Newsom, A., Byers, J., Meyer, J., Oyarzun, F., Lenihan, H., 2006. Invertebrate community responses to recreational clam digging. Mar. Biol. 149, 1489–1497.

Hamilton, D., Diamond, A., Wells, P., 2006. Shorebirds, snails, and the amphipod (Corophium volutator) in the upper Bay of Fundy: top–down vs. bottom–up factors, and the influence of compensatory interactions on mudflat ecology. Hydrobiologia 567, 285–306.

Hardege, J., Bentley, M., Beckmann, M., Müler, C., 1996. Sex pheromones in marine polychaetes: volatile organic substances (VOS) isolated from Arenicola marina. Mar. Ecol. Prog. Ser. 139, 157–166.

Hardege, J.D., Bentley, M.G., 1997. Spawning synchrony in Arenicola marina: evidence for sex pheromonal control. Proc. R. Soc. 264, 1041–1047.

Hermsen, J.M., Collie, J.S., Valentine, P.C., 2003. Mobile fishing gear reduces benthic megafaunal production on Georges Bank. Mar. Ecol. Prog. Ser. 260, 97–108.

Hitier, B., Ratiskol, G., L'Heveder, J., 2010. Evaluation de la fréquentation des zones de pêche à pied sur le littoral Loire-Bretagne. http://archimer.ifremer.fr/doc/00041/15232/.

Hixon, M.A., Tissot, B.N., 2007. Comparison of trawled vs untrawled mud seafloor assemblages of fishes and macroinvertebrates at Coquille Bank, Oregon. J. Exp. Mar. Biol. Ecol. 344, 23–34.

Hurlbert, S.H., 1990. Spatial distribution of the montane unicorn. Oikos 58, 257–271.

Hüttel, M., 1990. Influence of the lugworm Arenicola marina on porewater nutrient profiles of sand flat sediments. Mar. Ecol. Prog. Ser. 62, 241–248.

Illian, J., Penttinen, A., Stoyan, H., Stoyan, D., 2008. Statistical analysis and modelling of spatial point patterns (Statistics in practice). Wiley-Interscience, 560 pp.

Jennings, S., Dinmore, T.A., Duplisea, D.E., Warr, K.J., Lancaster, J.E., 2001. Trawling disturbance can modify benthic production processes. J. Animal Ecol. 73, 459–475.

Jennings, S., Nicholson, M., Dinmore, T., Lancaster, J., 2002. Effects of chronic trawling disturbance on the production of infaunal communities. Mar. Ecol. Prog. Ser. 243, 251–260.

Kristensen, E., 2001. Impact of polychaetes (Nereis spp. and Arenicola marina) on carbon biogeochemistry in coastal marine sediments. Geochem. Trans. 2, 92.

Kromkamp, J.C., Forster, R.M., 2006. Developments in microphytobenthos primary productivity studies. In: Kromkamp, J. (Ed.), Functioning of Microphytobenthos in Estuaries: Proceedings of the Colloquium, Amsterdam, 21–23 August 2003, Koninklijke Nederlandse Akademie van Wetenschappen Verhandelingen, Afd. Natuurk (Tweede Reeks), pp. 9–30.

Kuhnert, J., Veit-Köhler, G., Büntzow, M., Volkenborn, N., 2010. Sediment-mediated effects of lugworms on intertidal meiofauna. J. Exp. Mar. Biol. Ecol. 387, 36–43.

Lambert, G., Jennings, S., Kaiser, M., Hinz, H., Hiddink, J., 2011. Quantification and prediction of the impact of fishing on epifaunal communities. Mar. Ecol. Prog. Ser. 430, 71–86.

Legendre, P., Fortin, M., 1989. Spatial pattern and ecological analysis. Vegetation 80, 107–138.

Legendre, P., Legendre, L., 2012. Numerical Ecology. Elsevier, 880 pp.

Loosmore, N.B., Ford, E.D., 2006. Statistical inference using the G or K point pattern spatial statistics. Ecology 87, 1925–1931.

MacDougall, A.S., McCann, K.S., Gellner, G., Turkington, R., 2013. Diversity loss with persistent human disturbance increases vulnerability to ecosystem collapse. Nature 494, 86–89.

Marshall, S., Elliott, M., 1997. A comparison of univariate and multivariate numerical and graphical techniques for determining inter and intraspecifc feeding relationships in estuarine fish. J. Fish. Biol. 53, 526–545.

Mawhinney, K.M., Hicklin, P.W., Boates, J.S., 1993. A re-evaluation of the numbers of migrant Semipalmated Sandpipers, Calidris pusilla, in the Bay of Fundy during fall migration. Can. Field Nat. 107, 19–23.

McLusky, D., Elliott, M., 2004. The Estuarine Ecosystem: Ecology, Threats and Management. OUP Oxford, 224 pp.

Neubauer, P., Jensen, O.P., Hutchings, J.A., Baum, J.K., 2013. Resilience and recovery of overexploited marine populations. Science 340, 347–349.

Nielsen, O.Ie., Kristensen, E., Holmer, M., 2003. Impact of Arenicola marina (Polychaeta) on sediment sulfur dynamics. Aquat. Microb. Ecol. 33, 95–105.

Oksanen, L., 2001. Logic of experiments in ecology: is pseudoreplication a pseudoissue? Oikos 94, 27–38.

Percival, D.P., 1995. On estimation of the wavelet variance. Biometrika 82, 619–631.

Perry, G.L.W., Miller, B.P., Enright, N.J., 2006. A comparison of methods for the statistical analysis of spatial point patterns in plant ecology. Plant Ecol. 187, 59–82.

Perry, J.N., Liebhold, A.M., Rosenberg, M.S., Dungan, J., Miriti, M., Jakomulska, A., Citron-Pousty, S., 2002. Illustrations and guidelines for selecting statistical methods for quantifying spatial pattern in ecological data. Ecography 25, 578–600.

Piersma, T., Jukema, J., 1990. Budgeting the flight of a long-distance migrant changes in nutrient reserve levels of bar-tailed godwits at successive spring staging sites. Ardea 78, 315–337.

Piersma, T., Koolhaas, A., Dekinga, A., Beukema, J.J., Dekker, R., Essink, K., 2001. Long-term indirect effects of mechanical cockle-dredging on intertidal bivalve stocks in the Wadden Sea. J. Appl. Ecol. 38, 976–990.

Piersma, T., van Aelst, R., Kurk, K., Berkhoudt, H., Maas, L.R.M., 1998. A new pressure sensory mechanism for prey detection in birds: the use of principles of seabed dynamics? Proc. R. Soc. Biolog. Sci. Ser. B 265, 1377–1383.

Pinckney, J.L., Zingmark, R.G., 1993. Modeling the annual production of intertidal benthic microalgae in estuarine ecosystems. J. Phycol. 29, 396–407.

Ramos-Gómez, J., Martins, M., Raimundo, J., Vale, C., Laura Martín-Díaz, M., Ángel DelValls, T., 2011. Validation of Arenicola marina in field toxicity bioassays using benthic cages: biomarkers as tools for assessing sediment quality. Mar. Pollut. Bull. 62, 1538–1549.

Retraubun, A.S.W., Dawson, M., Evans, S., 1996. Spatial and temporal factors affecting sediment turnover by the lugworm Arenicola marina (L.). J. Exp. Mar. Biol. Ecol. 201, 23–35.

Riisgård, H.U., Banta, G.T., 1998. Irrigation and deposit feeding by the lugworm Arenicola marina, characteristics and secondary effects on the environment. A review of our current knowledge. Vie Milieu 48, 243–257.

Rijken, M., 1979. Food and food uptake in Arenicola Marina. J. Sea Res. 13, 406–410.

Ripley, B.D., 1976. The second-order analysis of stationary point processes. J. Appl. Probab. 13, 255–266.

Rodríguez-Romero, A., Khosrovyan, A., Del Valls, T.A., Obispo, R., Serrano, F., Conradi, M., Riba, I., 2013. Several benthic species can be used interchangeably in integrated sediment quality assessment. Ecotoxicol. Environ. Saf. 92, 281–288.

Rosenberg, M.S., Anderson, C.D., 2011. PASSaGE: pattern analysis, spatial statistics and geographic exegesis. Version 2. Meth. Ecol. Evol. 2, 229–232.

Rossi, F., Forster, R.M., Montserrat, F., Ponti, M., Terlizzi, A., Ysebaert, T., Middelburg, J.J., 2007. Human trampling as short-term disturbance on intertidal mudflats: effects on macrofauna biodiversity and population dynamics of bivalves. Mar. Biol. 151, 2077–2090.

Salinas, S., Perez, K.O., Duffy, T.A., Sabatino, S.J., Hice, L.A., Munch, S.B., Conover, D.O., 2012. The response of correlated traits following cessation of fishery-induced selection. Evol. Appl. 5, 657–663.

Sandulli, R., Pinckney, J., 1999. Patch sizes and spatial patterns of meiobenthic copepods and benthic microalgae in sandy sediments: a microscale approach. J. Sea Res. 41, 179–187.

Shephard, S., Brophy, D., Reid, D., 2010. Can bottom trawling indirectly diminish carrying capacity in a marine ecosystem? Mar. Biol. 157, 2375–2381.

Smith, B., Collie, J., Lengyel, N., 2013. Effects of chronic bottom fishing on the benthic epifauna and diets of demersal fishes on northern Georges Bank. Mar. Ecol. Prog. Ser. 472, 199–217.

Stoyan, D., Kendall, W.S., Mecke, J., 1995. Stochastic Geometry and its Applications. John Wiley & Sons Chichester, 436 pp.

Sutherland, T.F., Shepherd, P.C.F., Elner, R.W., 2000. Predation on meiofaunal and macrofaunal invertebrates by western sandpipers (Calidris mauri): evidence for dual foraging modes. Mar. Biol. 137, 983–993.

Tobler, W., 1970. A computer movie simulating urban growth in the Detroit region. Econ. Geogr. 46, 234–240.

Torrence, C., Compo, G.P., 1998. A practical guide to wavelet analysis. Bull. Am. Meteorolog. Soc. 79, 61–78.

Underwood, A.J., Chapman, M.G., 1996. Scales of spatial patterns of distribution of intertidal invertebrates. Oecologia 107, 212–224.

Veale, L.O., Hill, A.S., Hawkins, A.J.S., Brand, A.R., 2000. Effects on long-term physical disturbance by commercial scallop fishing on subtidal epifaunal assemblages and habitats. Mar. Biol. 137, 325–337.

Volkenborn, N., Hedtkamp, S.I.C., van Beusekom, J.E.E., Reise, K., 2007. Effects of bioturbation and bioirrigation by lugworms (Arenicola marina) on physical and chemical sediment properties and implications for intertidal habitat succession. Estuar. Coast. Shelf Sci. 74, 331–343.

Volkenborn, N., Reise, K., 2006. Lugworm exclusion experiment: responses by deposit feeding worms to biogenic habitat transformations. J. Exp. Mar. Biol. Ecol. 330, 169–179.

Watson, G.J., Bentley, M.G., Gaudron, S.M., Hardege, J.D., 2003. The role of chemical signals in the spawning induction of polychaete worms and other marine invertebrates. J. Exp. Mar. Biol. Ecol. 294, 169–187.

Whittaker, R.H., 1970. Communities and Ecosystems. Macmillan, New York.

Woodin, S.A., Lindsay, S.M., Wethey, D.S., 1995. Process-specific recruitment cues in marine sedimentary systems. Biol. Bull. 189, 49–58.

Zwarts, L.I., Blomert, A.-M., Hupkes, R., 1990. Increase of feeding time in waders preparing for spring migration from de Banc D'Arguin, Mauritania. Overdruk 436, 237–256.